Convenient Controllable Synthesis of Inorganic 1D Nanocrystals and 3D High-Ordered Microtubes

Zhenhui Kang,[a] Enbo Wang,*[a,b] Min Jiang,[a] Suoyuan Lian,[a] Yangguang Li,[a] and Changwen Hu[a]

Keywords: Nanotubes / Polyoxometalates / Synthetic methods

Polyoxometalates (POMs) nanorods, hollow particles, microtubes, and 3D-ordered tube systems were prepared using a novel and simple PEG/H_2O liquid system. POM nanorods with various diameters (30–400 nm) and lengths (500 nm to 2 μm) were produced in a well-controlled manner.

Introduction

Many interesting and technologically important phenomena occur in systems that have a spatial dimension similar to that of fundamental physical, chemical, or biological processes.[1] As a bridge between the molecular and the macroscopic world, mesosystems have become one of the most attractive subjects in physics, materials science, chemistry, and biology.[1] Nanosystems with characteristic lengths between 1 and 100 nm exhibit fascinating properties, such as quantized excitation, coulomb blocking, single-electron tunneling (SET), and metal−insulator transitions.[1] One-dimensional (1D) nanomaterials are of great fundamental and practical interest owing to their novel properties, which depend on their particular sizes and shapes.[1] Recently, much attention has been paid to the construction of advanced materials with such nanoscale building blocks.[2] Therefore, the exploration of preparation methods to control the sizes and shapes of nanomaterials is one of the focuses for the development of nanotechniques.[2−4]

A number of methods have been employed for the preparation of 1D nanomaterials, including template-assisted,[5] vapor-liquid-solid-(VLS-)assisted,[6] and electrochemical processes.[7] For most of these strategies, however, complicated process control, high reaction temperature, and long synthesis time are required. Recently, the introduction of microemulsions (or reverse micelles) has provided a relatively simple and powerful method for controlling the size, shape, and surface texture of nanoparticles and nanorods. In such microenvironments, the nanomaterials are encapsulated in the closed shells of surfactant molecules. The size and shape of nanoclusters can be well controlled by the size of the capsules, which can be controlled by changing the ratios of water and oil.[8] From this model of reaction fields, we speculate that if the closed capsules composed of surfactant molecules could be opened in one direction, a linear reaction field could be formed and a 1D nanomaterial could grow in such a microenvironment. Based on this speculation, we chose the nonionized surfactant polyethylene glycol (PEG) mixed with water so as to form a linear reaction field and explore the controllable synthesis of polyoxometalate (POM) nanocrystals and their nano/microstructure material forms.

As one of the typical inorganic metal oxide clusters, POMs have recently received much attention owing to their novel compositions, structures, and applications in the fields of catalysis, pharmacology, electronic, and magnetic materials.[9,12] They can be regarded as extremely versatile inorganic entities for the construction of functionally active solids and are one of the favorite candidates to be transformed into nanometer-sized materials.

It is noteworthy that POMs are nanosized polyoxometalate clusters that form by a self-assembly process in solution and can be isolated as solids. They have unique physicochemical properties such as strong Brønsted acidity, reversible multielectron redox transformations, activation of molecular oxygen and hydrogen peroxide, high proton mobility across their discrete ionic structure, etc.[9] These properties make POMs promising acid, redox, and bifunctional catalysts in homogeneous and heterogeneous systems. POMs are widely used as model systems for fundamental research, providing unique opportunities for mechanistic studies on

---

[a] Institute of Polyoxometalate Chemistry, Department of Chemistry, Northeast Normal University,
Changchun, Jilin 130024, P. R. China
Fax: (internat.) + 86-431/568-4009
E-mail: wangenbo@public.cc.jl.cn
[b] Institute of Coordination Chemistry, State Key Laboratory Nanjing University,
Nanjing, Jiangsu 210093, P. R. China

the molecular level. They have also become increasingly important for applied catalysis. Several new industrial processes based on POM catalysis have been commercialized.[12k] Current studies of catalysis by POMs and related systems concentrate on the catalyst preparation, characterization and monitoring, mechanistic aspects, application for organic synthesis and fine and specialty chemicals, and alkane activation. Other topics of interest include the design of advanced solid acid catalysts based on POMs incorporated into mesoporous zeolites.[9,12] POM crystalline nanomaterials, especially nano/microtubes and their 3D-ordered systems, will provide an opportunity to explore their unique properties on catalysis in many fields.

Müller et al.[10] have ingeniously synthesized many giant clusters of POMs on the nanometer scale, including novel kinds of large rings and wheel-shaped systems with 176 or even more Mo atoms. Recently, Misono et al. have studied the growth process of polyoxotungstate $(NH_4)_3PW_{12}O_{40}$ crystalline nanoparticles.[11] However, the rational design and controllable preparation of POM-based crystalline nanomaterials are still huge challenges. Because numerous well-characterized POMs are available,[12] it is extremely important to develop new strategies for the preparation of POM nanocrystals and nano/micro systems to explore their novel properties.

In this paper, we report on the 1D POM crystalline nanorods, hollow particles, nano/microtubes and 3D high-ordered tube systems prepared by a convenient and novel controllable synthesis method. Both the size and shape of these POM crystalline nanorods can be controlled by the use of different kinds of PEG and various volumes of water.

Results and Discussion

POMs Crystalline Nanorods

In our experiments, $AgNO_3$ (0.25 g) and $H_4SiW_{12}O_{40}·nH_2O$ (1 g) were dissolved in a mixture of two different PEG/H_2O systems, one with $w = 2.5:1$ and the other with $w = 2.5:2.5$ ($w = [PEG]/[H_2O]$). Both of the systems were stirred before to give transparent sticky fluids. After the two systems were mixed, the reaction mixture remained clear. However, a large amount of white flocculent precipitate formed when a fourfold excess of ethanol was added. Element analysis of the white products give a molar ratio of Ag/Si/W = 4:1:12. The FT-IR spectrum exhibits characteristic peaks at 1100, 1011, 970, 919, 882, and 795 cm^{-1}, which are attributed to the ν(Si=Oa), ν(W=Ot), ν(W−Ob−W), and ν(W−Oc−W) absorptions of a Keggin-type structure, respectively. Transmission electron microscopy (TEM) images of samples taken from the PEG-400/H_2O ($w = 2.5:1.5$) system showed $Ag_4SiW_{12}O_{40}$ nanorods with a regular shape and size (Figure 1, a and c). The electron diffraction (Figure 1, b) and XRD patterns (Figure 1, d) confirm that these $Ag_4SiW_{12}O_{40}$ nanorods are crystalline.

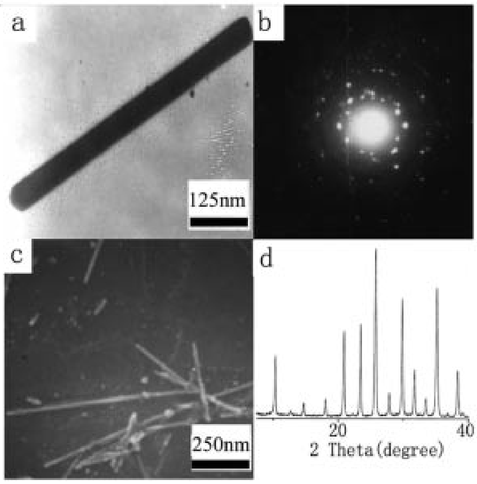

Figure 1. (a) TEM image of $Ag_4SiW_{12}O_{40}$ nanorods taken from the PEG-400/H_2O ($w = 2.5:1.5$) system; (b) electron diffraction pattern of the nanocrystals of $Ag_4SiW_{12}O_{40}$; (c) SEM image of $Ag_4SiW_{12}O_{40}$ nanorods; (d) XRD patterns of $Ag_4SiW_{12}O_{40}$ nanorods

In these experiments, the surfactant PEG molecules act as the most important component introduced into the reaction system. It is known that the nonionized surfactant PEG molecules form chain-like structures due to the assembly in water.[13] Therefore, we can imagine that many 1D liquid reaction fields could be formed when the PEG and a small amount of water are mixed together. The metathetical reactions of $AgNO_3$ and $H_4SiW_{12}O_{40}·nH_2O$ and the growth of $Ag_4SiW_{12}O_{40}$ nanoclusters are strictly limited in such divided linear reactions along the directional space. Owing to the inhibition of surfactant PEG, further agglomeration will be stopped and the nanorods are therefore formed and fixed in the linear environments. Scheme 1 illustrates the possible mechanism. The TEM images of POM nanorods shown in Figure 2 proved these assumptions to be correct. Nanorods with various regular sizes and shapes can be prepared in different PEG/H_2O systems.

It is noteworthy that different molecular masses of PEG molecules lead to a variety of lengths of nanorods. Lower molecular weight surfactant of PEG-400 could be selected to prepare shorter POM nanorods with average lengths of 500−800 nm. PEG-600, which has a higher molecular weight, could be used to synthesize longer POM nanorods with average lengths of 1−2 μm. Figure 2, a and b, show the nanorods produced by the PEG-400/H_2O systems. Figure 2, c and d, illustrate the nanorods prepared by the PEG-600/H_2O systems. With increasing molecular mass of PEG, the length of the linear reaction fields is probably greater, and thus the size of nanorods is increased. Therefore, the length of POM nanorods can be controlled by adjustment of the molecular weight of PEG.

We further showed that the content of water in the preparation of 1D POM nanomaterials has a direct influence on the diameter of the nanorods. The relationship between

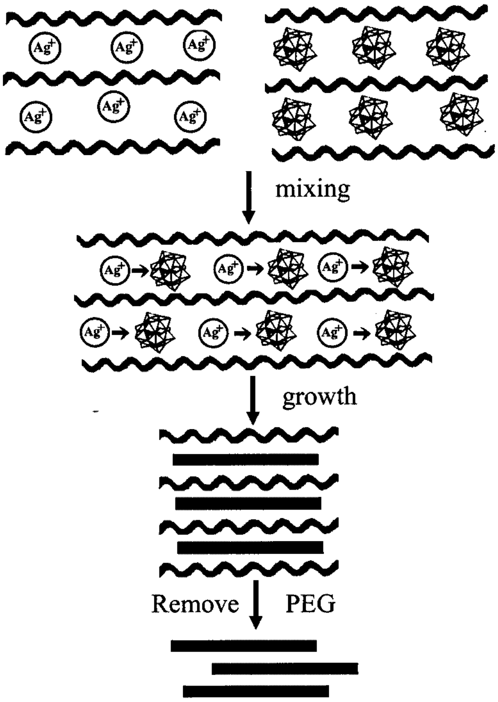

Scheme 1. Schematic diagram of the proposed formation process of POM nanorods

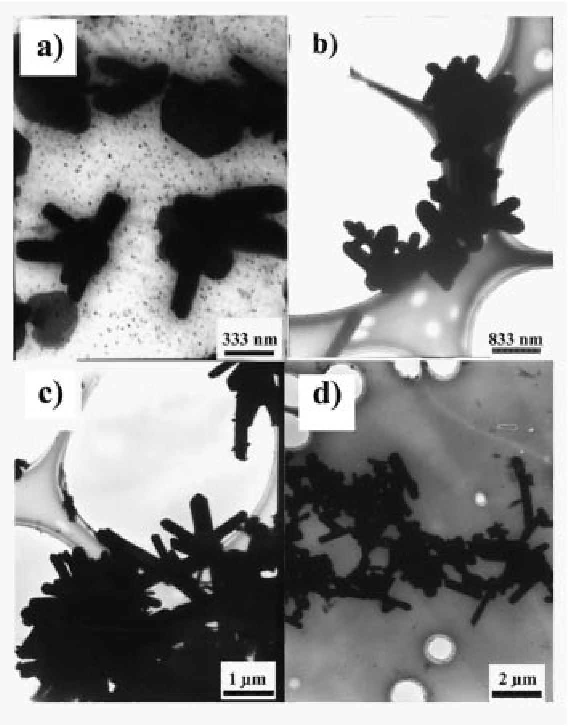

Figure 2. TEM images of $Ag_4SiW_{12}O_{40}$ nanorods with a length of: (a) and (b) 500−800 nm in the PEG-400/H_2O system; (c) and (d) 1−2 µm in the PEG-600/H_2O system

the size of 1D POM nanomaterials and the content of water is shown in Table 1. It is noteworthy that the diameter of the nanorods increases with increasing water content. As noted above, in this liquid system, many linear reaction fields exist, and the nanorods can be formed and fixed there. With the addition of water, the linear reaction field, i.e. the reaction space, will become larger, and thus the nanorods will also have larger diameters. Figure 3 shows nanorods with different diameters prepared in PEG-400/H_2O systems containing different amounts of water. Their diameters vary with the content of water in PEG-400/H_2O systems, namely 30, 70, and 90 nm for (a) PEG-400/H_2O = 2.5:1.0, (b) PEG-400/H_2O = 2.5:1.5, and (c) PEG-400/H_2O = 2.5:2.0, respectively. Similar results are also found in the PEG-600/H_2O (w = 2.5:1.5, 2.5:2.0, 2.5:2.5) systems (as shown in Figure 4), in which nanorods with diameters of (a) 200 nm, (b) 300 nm, and (c) 400 nm are obtained, respectively. Figure 5 shows the SEM images of POM nanorods with different diameters and lengths.

Table 1. Influence of the amount of water in PEG/H_2O systems on the diameters of the POM 1D nanomaterials

Surfactants	$Ag_4SiW_{12}O_{40}$ nanorods/nanowires [nm]	Content of water PEG/H_2O [mL/mL]
PEG-400	30	2.5:1.0
	70	2.5:1.5
	90	2.5:2.0
PEG-600	200	2.5:1.5
	300	2.5:2.0
	400	2.5:2.5

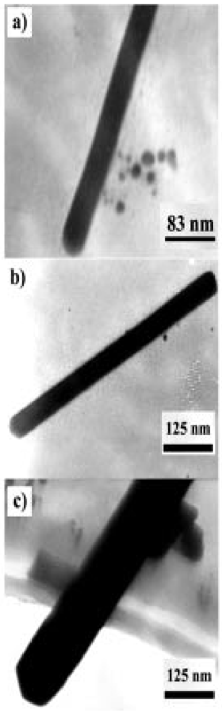

Figure 3. TEM images of nanorods taken from the PEG-400/H_2O systems; the diameters of these nanorods vary with the amount of water, namely 30, 70, and 90 nm for (a) PEG-400/H_2O = 2.5:1.0; (b) PEG-400/H_2O = 2.5:1.5; (c) PEG-400/H_2O = 2.5:2.0 (mL/mL)

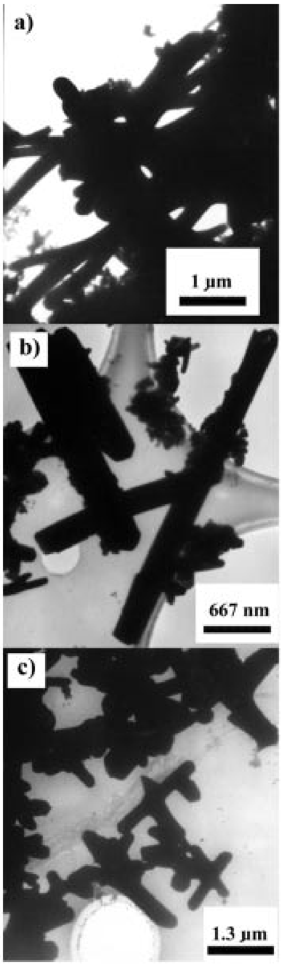

Figure 4. TEM images of nanorods taken from the PEG-600/H_2O systems; the diameters of these nanorods vary with the amount of water, namely 200, 300, and 400 nm for (a) PEG-600/H_2O = 2.5:1.5; (b) PEG-600/H_2O = 2.5:2.0; (c) PEG-600/H_2O = 2.5:2.5 (mL/mL)

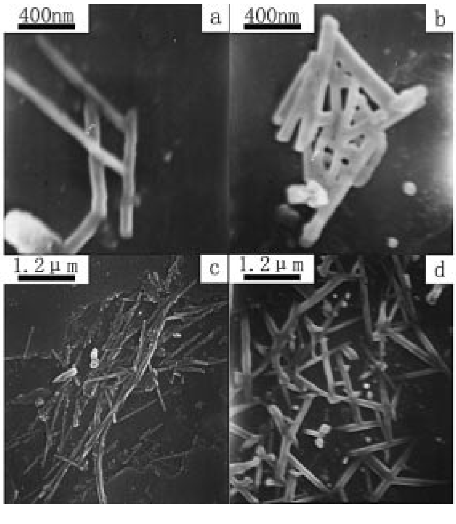

Figure 5. SEM images of POM nanorods with different diameters and lengths

In order to investigate the action of PEG in this liquid system, control experiments without PEG addition were carried out. Figure 6, a−c, show the SEM images of $Ag_4SiW_{12}O_{40}$ particles with a diameter of about 5 μm. Figure 6, d, is the XRD pattern of $Ag_4SiW_{12}O_{40}$ particles. From this figure we can see that the products are huge particles in the ordinary liquid system, hence PEG is a very important factor in controlling the shape and size of products.

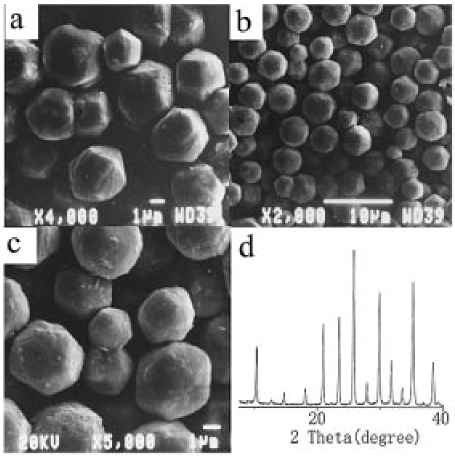

Figure 6. SEM images and XRD pattern of $Ag_4SiW_{12}O_{40}$ particles

In this liquid system, the reaction process was analyzed by conductometry. Figure 7 shows the relationship between the time and the conductivity in the PEG-400/H_2O (w = 2.5:1.5) system. Curve (a) shows the conductivity during the reaction when the solution containing PEG, water, and $AgNO_3$ was added to the other solution containing PEG, water, and $H_4SiW_{12}O_{40}$. Curve (b) shows the conductivity during the reaction when the solution containing PEG, water, and $H_4SiW_{12}O_{40}$ was added to the other solution containing PEG, water, and $AgNO_3$. Because of the coordination action between the Ag^+ and O atom in the PEG, the conductivity of the solution containing PEG, water, and $AgNO_3$ is lower than the solution that contains PEG, water, and $H_4SiW_{12}O_{40}$. When the reaction happens in the linear reaction fields, the formation of $Ag_4SiW_{12}O_{40}$ nanocrystals leads to a decrease of the electrolyte concentration. Thus, the conductivity of the reaction system decreases with the growth of nanocrystals. Curve (b) exhibits a sharp rise at the beginning of the reaction. This is due to the fact that the solution containing PEG, water, and $H_4SiW_{12}O_{40}$ has a higher conductivity than that of the solution that contains PEG, water, and $AgNO_3$.

According to these experimental results, these liquid-phase reactions can be regarded as a method that can be used to control the length and diameter of 1D POM nanomaterials rationally and effectively. During the preparation of 1D POM nanomaterials, the sticky solution, in which the uniform POM nanorods and/or nanowires could be obtained and exist stably without further agglomeration, is one of the important factors.

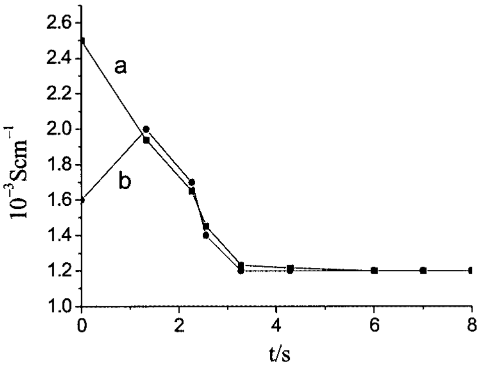

Figure 7. Relationship between the time and the conductivity

POM Hollow Particles

We wanted to produce short POM nanorods by means of the PEG-200/H_2O system, but, hollow particles were obtained instead of the expected short nanorods. This result can be attributed to the following. PEG assembly structures in water are flexible and chain-like. Surfactant PEG with lower molecular weight becomes more flexible and looser aggregates form. For PEG-200, the aggregates in water are different from those that form with higher molecular weight PEGs. The aggregates of PEG 200 in water are so soft that they cannot template the synthesis of POM nanorods. Thus, the soft and crimped aggregates lead to the formation of hollow particles. The diameters of these hollow particles are about 800 nm with homogeneous wall thickness (70 nm). Typical SEM images of hollow POM particles are shown in Figure 8. As noted above, many unique properties make POMs promising acid, redox, and bifunctional catalysts in homogeneous and heterogeneous systems. These hollow POM particles could be useful in a rich variety of applications. For instance, they may be suggested or demonstrated as extremely small containers for microencapsulation − a process that plays an important role in many areas such as catalysis, delivery of drugs, development of artificial cells, and protection of biologically active materials (e.g., enzymes, proteins, or deoxyribonucleic acids, DNAs).[14]

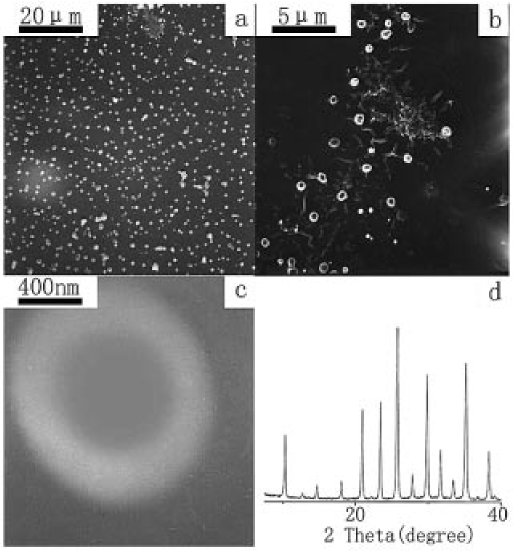

Figure 8. SEM images and XRD pattern of hollow $Ag_4SiW_{12}O_{40}$ particles

POM Microtubes and a 3D Ordered Microtube System

We can imagine that many 1D liquid reaction fields can be formed when PEG and a small quantity of water are mixed together. The larger the amount of water, the broader the reaction fields become. If the reaction fields are so broad that they can embrace the PEG aggregate then cannular structures may be obtained from PEG/H_2O systems. Figure 9, a, shows the half-tube obtained when PEG-400/H_2O = 2.5:3.5 (mL/mL) was used. Whole microtubes (shown in Figure 9, b−f) with diameters of about 700 nm were obtained using PEG-400/H_2O = 2.5:5 (mL/mL). Here, another important factor is the speed of stirring. High-speed stirring leads to the degradation of POM microtubes. On the contrary, well-grown microtubes were prepared at low stirring speeds (shown in Figure 9, d−f).

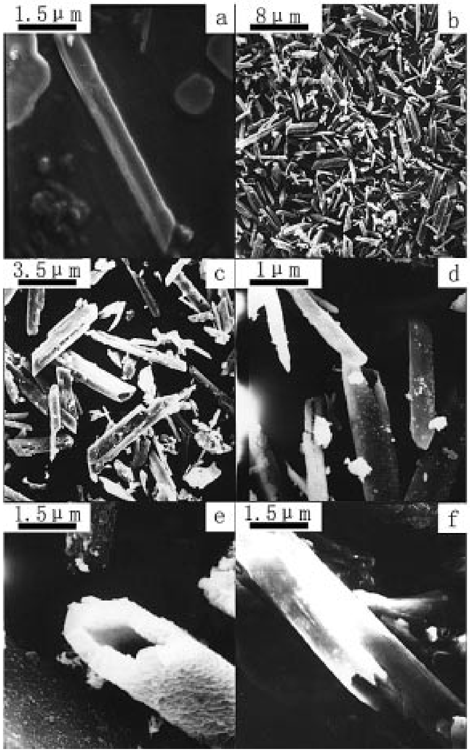

Figure 9. SEM images of $Ag_4SiW_{12}O_{40}$ microtubes

During the course of preparing the microtubes, an interesting phenomenon (shown in Figure 10, a) was observed: several microtubes fused together. So, we have developed a low-temperature controlled hydrothermal method using PEG/H_2O systems to synthesize 3D highly ordered microtunnel arrays. We mixed an $AgNO_3$/PEG/H_2O system and an $H_4SiW_{12}O_{40}$/PEG/H_2O system and then stirred slowly in order to make the mixture homogeneous. Then, the mixture was sealed in a 25-mL Teflon-lined reactor, with 70% filling, and heated at about 70 °C for 72 h. Figure 10, b and c, show the SEM images of 3D-ordered microtunnel POM materials with diameters of about 1 μm. These ordered tunnels may be used as a microreactor. They should be useful in various applications, such as catalysis, selective delivery, and template for the synthesis of nanostructure materials.

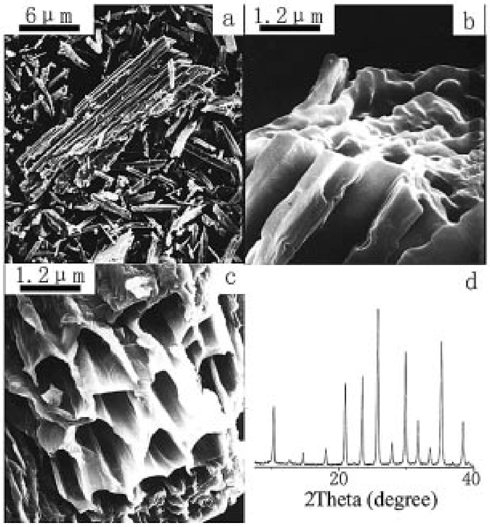

Figure 10. SEM images and XRD pattern of $Ag_4SiW_{12}O_{40}$ 3D-ordered microtubes

Figure 11 shows N_2 adsorption isotherms of the hollow particles, microtubes, and 3D-ordered tubes. In these systems there are many very large cavities. These isotherms have the typical shape of large porous materials.

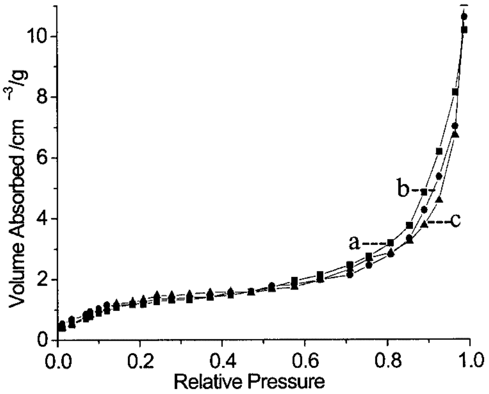

Figure 11. Isotherms of N_2 adsorption at 77 K: (a) hollow particles; (b) microtubes; (c) 3D-ordered tubes

Conclusion

In conclusion, the novel, and simple liquid PEG/H_2O system was applied in the preparation of POM nanorods, hollow particles, microtubes, and 3D-ordered tube systems. A possible mechanism is that chain-like PEG molecules segment the liquid reaction fields to form many linear microenvironments, in which the interaction of reactants and the growth of nanomaterials are limited in the directional space. From this reaction model, we presume that many other 1D nanomaterials such as metal salts ($BaSO_4$, CdS) and metal oxides (ZnO, CuO, Fe_3O_4) could also be prepared.

Furthermore, 1D POM nanorods, hollow particles, microtubes, and 3D-ordered tube system have been prepared. The regular sizes and shapes are well controlled by the PEG/H_2O systems. Owing to the extensive applications of POMs in catalysis, medicine, and functional materials, the preparation of POM nanostructured materials could provide a new route to explore their excellent properties.

Experimental Section

General: All reagents were purchased from commercial suppliers and used without further purification. The SEM images were obtained with a JEOL JSM-840 operating at 20 kV. The XRD patterns were obtained with a Rigaku D/max 2500V PC diffractometer with Cu-K_α radiation. A JEM-2010 transmission electron microscope was used to examine the morphology of the POMs nanocrystals.

General Preparation of $Ag_4SiW_{12}O_{40}$ Nanorods: $H_4SiW_{12}O_{40}\cdot nH_2O$ (1 g) was dissolved in a mixture of PEG-400 (or PEG-600)/H_2O (2.5 mL/1 mL, about 2.5 mL of the mixture) whilst stirring to give a clear and homodisperse system. Another 2.5 mL of PEG-400 (or PEG-600), mixed with 1−2 mL of H_2O and 0.23 g of $AgNO_3$, was stirred until it became clear. The above two solutions were then mixed and stirred for 1 min. Then, a fourfold excess of ethanol was added to form a white precipitate. The white precipitate was centrifuged, washed with ethanol, and dried in air at 50 °C for 1 h. The yield was 90% ($Ag_4SiW_{12}O_{40}$, 1.14 g, based on W). A similar approach was used for the synthesis of POM hollow particles using the PEG-200/H_2O (2.5 mL/1.5 mL) system. A clear and homodisperse system of $AgNO_3$/PEG-200/H_2O (0.5 g/2.5 mL/1.5 mL) and a similar system of $H_4SiW_{12}O_{40}$/PEG-200/H_2O (0.5 g/2.5 mL/1.5 mL) were prepared according to the above procedure. Then, the two systems were mixed and stirred. A fourfold excess of ethanol was added to form a white precipitate. The white precipitate was also centrifuged, washed with ethanol, and dried in air at 50 °C for 1 h. A very similar approach was employed to prepare the $Ag_4SiW_{12}O_{40}$ microtubes. A large amount of water (PEG/H_2O = 1:2) was added to the reaction system, with slow stirring. This mixture was sealed in a 25-mL Teflon-lined reactor, with 70% filling, and heated to about 70 °C for 72 h, to give the 3D-ordered microtube arrays.

Acknowledgments

This work was financially supported by the National Natural Science Foundation of China (20171010).

---

[1] [1a] Y. N. Xia, J. A. Rogers, K. E. Paul, G. M. Whitesides, *Chem. Rev.* **1999**, *99*, 1823−1848. [1b] X. F. Duan, Y. Huang, Y. Cui, J. F. Wang, C. M. Lieber, *Nature* **2001**, *409*, 66−69. [1c] M. H. Huang, S. Mao, H. Feick, H. Q. Yan, Y. Y. Wu, H. Kind, E. Weber, R. Russo, P. D. Yang, *Science* **2001**, *292*, 1897−1899.

[2] V. F. Puntes, K. M. Krishnan, A. P. Alivisatos, *Science* **2001**, *291*, 2115−2117, and references therein.

[3] M. Li, H. Schnablegger, S. Mann, *Nature* **1999**, *402*, 393−395.

[4] R. Y. Wang, J. Yang, Z. P. Zheng, M. D. Carducci, J. Jiao, S. Seraphin, *Angew. Chem. Int. Ed.* **2001**, *40*, 549−552.

[5] B. R. Martin, D. J. Dermody, B. D. Resis, M. M. Fang, L. A.

Lyon, M. J. Natan, T. E. Mallouk, *Adv. Mater.* **1999**, *11*, 1021−1025.

[6] J. T. Hu, T. W. Odom, C. M. Lieber, *Acc. Chem. Res.* **1999**, *32*, 435−445.

[7] M. B. Mohamed, K. Z. Ismail, S. Link, M. A. El-Sayed, *J. Phys. Chem. B* **1998**, *102*, 9370−9374.

[8] [8a] S. Vaucher, M. Li, S. Mann, *Angew. Chem. Int. Ed.* **2000**, *39*, 1793−1796. [8b] J. D. Hopwood, S. Mann, *Chem. Mater.* **1997**, *9*, 1819−1828. [8c] M. A. López-Quintela, J. Rivas, *J. Colloid Interface Sci.* **1993**, *158*, 446−451.

[9] [9a] M. T. Pope, A. Müller, *Angew. Chem. Int. Ed. Engl.* **1991**, *30*, 34−48. [9b] A. Müller, F. Petters, M. T. Pope, D. Gatteschi, *Chem. Rev.* **1998**, *98*, 239−272. [9c] J. T. Rhule, C. L. Hill, D. A. Judd, R. F. Schinazi, *Chem. Rev.* **1998**, *98*, 327−357. [9d] E. Coronado, C. J. Gomez-Garcia, *Chem. Rev.* **1998**, *98*, 273−296. [9e] N. Mizuno, M. Misono, *Chem. Rev.* **1998**, *98*, 199−217.

[10] [10a] A. Müller, S. Q. N. Shah, H. Bogge, M. Schmidtmann, *Nature* **1999**, *397*, 48−50. [10b] A. Müller, S. K. Das, P. Kögerler, H. Bögge, M. Schmidtmann, A. X. Trautwein, V. Schünemann, E. Krickemeyer, W. Preetz, *Angew. Chem. Int. Ed.* **2000**, *39*, 3413−3417.

[11] T. Ito, K. Inumaru, M. Misono, *Chem. Mater.* **2001**, *13*, 824−831.

[12] [12a] L. H. Bi, E. B. Wang, J. Peng, R. D. Huang, L. Xu, C. W. Hu, *Inorg. Chem.* **2000**, *39*, 671−679. [12b] W. S. You, E. B. Wang, Y. Xu, Y. G. Li, L. Xu, C. W. Hu, *Inorg. Chem.* **2001**, *40*, 5468−5471. [12c] L. H. Bi, R. D. Huang, J. Peng, E. B. Wang, Y. H. Wang, C. W. Hu, *J. Chem. Soc., Dalton Trans.* **2001**, 121−129. [12d] Y. H. Guo, E. B. Wang, Y. N. Zhou, S. H. Feng, *Chem. Mater.* **2000**, *12*, 3501−3508. [12e] Y. H. Guo, C. W. Hu, X. L Wang, E. B. Wang, Y. N. Zhou, S. H. Feng, *Chem. Mater.* **2001**, *13*, 4058−4064. [12f] L. Xu, Y. Q. Sun, E. B. Wang, E. H. Shen, Z. R. Liu, C. W. Hu, *New J. Chem.* **1999**, *23*, 1041−1044. [12g] Y. H. Guo, D. F. Li, C. W. Hu, Y. H. Wang, E. B. Wang, *Appl. Catal. B (Environment)* **2001**, *30*, 337−349. [12h] J. Peng, W. Z. Li, E. B. Wang, Q. L. Bai, *J. Chem. Soc., Dalton Trans.* **2001**, 3668−3671. [12i] C. W. Hu, Q. L. He, Y. H. Zhang, Y. Y. Liu, Y. F. Zhang, Y. D. Tang, J. Y. Zhang, E. B. Wang, *Chem. Commun.* **1996**, 121−122. [12j] W. S. You, Y. B. Wang, E. B. Wang, L. Xu, C. W. Hu, X. Q. Xin, F. Li, *Chem. J. Chin. Univ.* **2000**, *21*, 1636−1638. [12k] E. B. Wang, C. W. Hu, L. Xu, *Concise course of polyoxometalates chemistry [M]*, Chemical Industry Press, Beijing, **1997**, pp. 170−211.

[13] [13a] J. H. Sun, Y. J. Gong, W. H. Fan, Y. H. Sun, *Chem. J. Chin. Univ.* **2000**, *21*, 95−99, and references therein. [13b] W. Z. Wang, Y. J. Zhan, G. H. Wang, *Chem. Commun.* **2001**, 727−728.

[14] Y. Lu, Y. D. Yin, Y. N. Xia, *Adv. Mater.* **2001**, *13*, 271−274.

Received June 9, 2002
[I02302]